

# Trap dominated dynamics of classical dimer models

Dibyendu Das, Jané Kondev and Bulbul Chakraborty

*Martin Fisher School of Physics, Brandeis University, Mailstop 057, Waltham, Massachusetts 02454-9110, USA*

We consider dynamics of classical dimer models undergoing a phase transition to an ordered, frozen state. Relaxation processes are dominated by traps which are entropic in origin and can be traced to the locally jammed nature of the dimer states. Depending on the nature of the phase transition, critical dynamics are characterized either by an exponential, or sub-exponential in time relaxation of the order parameter. In the latter case relaxation time scales diverge *exponentially* as the critical point is approached, following the Vogel-Fulcher law.

A variety of systems such as supercooled liquids, colloids, granular matter and foams, exhibit a transition from a flowing fluid phase to a frozen solid phase. Jamming due to spatial constraints imposed on the elementary constituents of these materials has been proposed as a possible common cause of this dynamical arrest [1–3]. Model systems, such as hard spheres, have an important role to play in the investigation of such a scenario since they allow for a precise definition of jamming [4]. They are also useful in elucidating the precise relationship between thermodynamics and dynamics in materials exhibiting a jammed phase [5].

Dimer models are examples of jammed systems which have the added advantage of being exactly solvable [6]. States of the dimer model are specified by placing dimers on the bonds of the lattice so that every site is covered by exactly one dimer; see Fig 1. These dimer coverings are “locally jammed” [4] as each dimer cannot move to an empty neighboring bond without violating the packing constraint. Moves that involve *loops* of dimers and adjacent empty bonds, on the other hand, are allowed. An example of such a move for the hexagonal lattice involving an elementary plaquette is shown in Fig. 1a. (Stochastic dynamics of the dimer model on the square lattice based on these elementary moves were considered by Henley [7].) Most states of the dimer model allow for elementary moves; an example of one which does not is shown in Fig. 1b. The smallest change in this case involves a system spanning loop, and we call this state “maximally jammed”. If we define an energy functional on the space of dimer coverings which favors the maximally jammed state, a transition into this state will occur as we lower the temperature. The central question we address in this letter is: *What happens to relaxation time scales of the dimer model as the transition to the maximally jammed state is approached?* We will show that the relaxation is dominated by entropy barriers and is sensitive to the thermodynamics of the model near the phase transition point.

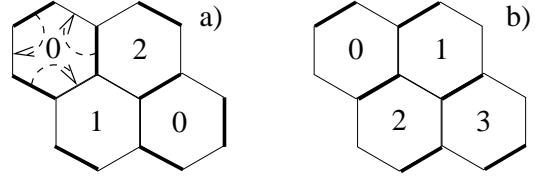


FIG. 1. (a) Dimer covering of the honeycomb lattice with an elementary loop update indicated by the arrows. The numbers are the heights of the equivalent interface. (b) An ordered, maximally jammed dimer covering; the equivalent interface is tilted with maximum slope.

We consider two energy functionals. One leads to a Pokrovsky-Talapov type transition to the maximally jammed state [6]. The other exhibits a continuous transition to the same state along a metastable line, and belongs to a different universality class. For both transitions we find strong departures from the canonical critical-slowness scenarios [8] due to the presence of entropy barriers. Barriers can be traced directly to the non-local nature of the dynamical moves allowed by the jammed states. For the transition that occurs along a metastable line, time scales associated with critical fluctuations diverge exponentially following a Vogel-Fulcher-like form. This is reminiscent of what is observed in fragile glass formers [9]. To our knowledge this is the first example of a system with no quenched in disorder which exhibits this type of critical dynamics.

*a. Dimer models* We consider the dimer model on the 2-d hexagonal lattice of linear size  $L$ , having  $2L^2$  sites and  $3L^2$  bonds, with periodic boundary conditions [10]. A useful representation of the dimer model is given by the height map which associates a discrete interface  $h(x, y)$  with every dimer covering [11]. The heights of the interface are defined on the vertices of the dual triangular lattice. The height difference  $\Delta$  between two nearest neighboring sites is  $-2$  or  $+1$  depending on whether the bond of the honeycomb lattice that separates them is occupied by a dimer or not; see Fig. 1a. Directions in which the height change is  $+\Delta$  are specified by orienting all the up pointing triangles of the dual lattice clockwise.

The dimer model has an extensive entropy. The ensem-

ble of equal weighted dimer coverings maps to a rough surface with a gradient-square free energy [11]. Fluctuations of the surface are entropic in origin. A phase transition can be induced in the dimer model by including an energy functional which is minimized by a dimer covering corresponding to a smooth, *maximally tilted* surface which corresponds to the maximally jammed state shown in Fig. 1b. Here we discuss two such energy functionals.

For periodic boundary conditions the tilt vector,  $(\Delta_x h, \Delta_y h)$ , where  $\Delta_{x,y} h$  is the average height difference in the  $x$  or  $y$  direction, has only one independent component  $\rho$  [12]. In terms of  $\rho$ , the energy functionals can be written as:

$$E(\rho) = \begin{cases} -(\mu L^2/3) & (1 + 8\rho^2) & (I) \\ -(\mu L^2/3) & (1 + 2\rho) & (K) \end{cases} ; \quad (1)$$

$\mu$  is a dimensionless coupling that drives the transition.

The entropy of the dimer model as a function of  $\rho$  was calculated exactly [10,13]:

$$S(\rho) = L^2 \left\{ \frac{2 \ln 2}{3} (1 - \rho) + \frac{2}{\pi} \int_0^{\frac{\pi}{2}(1-\rho)} dx \ln[\cos x] \right\} \quad (2)$$

This function has a maximum at  $\rho = 0$  which is the equilibrium value at  $\mu = 0$ . For finite  $\mu$  the  $I$  model was previously considered in Ref. [14], while the  $K$  model was solved by Kasteleyn [10].

In the  $I$  model, with the free energy  $F = E - S$ , and the energy and entropy given by Eqs. 1 and 2, there is an interesting phase transition along the metastable line, when the order parameter is confined to the free energy well around the zero-tilt state. Namely, at  $\mu_* = \pi/(8\sqrt{3})$  (the end-point of the metastable line) the order parameter  $\rho$  has a discontinuous jump from 0 to 1, characteristic of a first-order transition. At the same time, as  $\mu_*$  is approached from below, fluctuations of  $\rho$  around 0 diverge, as would be expected at a critical point. This transition was discussed in detail in Ref. [14].

By contrast, in the  $K$  model, there is a continuous variation of the equilibrium value of the order parameter,  $\rho_{min}$ , with  $\mu$ . On varying  $\mu$  from 0 to the transition point  $\mu_* = \ln 2$ ,  $\rho_{min}$  varies from 0 to 1. Apart from the shift of the free energy minimum, the fluctuations also grow with increasing  $\mu$ , and at the transition, the curvature of the free energy at its minimum goes to zero.

*b. Coarse-grained dynamics* As mentioned in the introduction, the hard constraint of non-overlapping of dimers, gives rise to nonlocal dynamics. We consider Monte-Carlo dynamics based on loop updates with loops of arbitrary size; a concrete implementation is given in Ref. [15]. Since we take periodic boundary conditions, loops with different winding numbers can be formed. We restrict loop updates to loops with winding numbers  $(0,0)$ ,  $(1,0)$  and  $(0,1)$ , only. The microscopic transition rates for loop updates are given by Metropolis rules that follow from Eq. 1.

Given the microscopic loop dynamics, which satisfy conditions of ergodicity and detailed balance, we ask what are the coarse-grained dynamics of the order parameter,  $\rho$ . Since the energy functions in Eq. 1 depend on the global tilt  $\rho$  only, it follows that all updates of topologically trivial loops (i.e. those with  $(0,0)$  winding number) have  $\Delta E = 0$ . Only when system spanning loops with nonzero winding numbers are updated does the energy of the state change [16]. This feature naturally leads to fast and slow processes in the Monte-Carlo dynamics. On a faster time scale, non-winding loops are updated with no effect on the overall tilt of the surface, while on a much slower time scale, winding loops are updated causing a change in the tilt of the surface.

The *coarse-grained* dynamics of global tilt changes are described by a master equation, which features an unusual form for the transition rates between different tilt states. Namely, the rates of transitions from higher into lower tilt states are determined by the energy barrier alone:

$$W_{\rho-1/L, \rho} = \Gamma_o e^{-(E(\rho-1/L) - E(\rho))} ; \quad (3)$$

here  $\Gamma_o$  is a constant. This follows from the observation that in order to lower the tilt and increase the energy an existing system spanning loop needs to be updated.

From detailed balance,  $W_{\rho-1/L, \rho}/W_{\rho, \rho-1/L} = \exp[-(F(\rho-1/L) - F(\rho))]$ , we conclude that the rates of transitions to higher tilt states must be determined by the entropy:

$$W_{\rho, \rho-1/L} = \Gamma_o e^{-(S(\rho-1/L) - S(\rho))} . \quad (4)$$

Eq. 4 can also be argued from the following observation: to increase the tilt and lower the energy, a new system-spanning loop has to be accommodated by (typically) many rearrangements of the topologically trivial loops. Once a new system spanning loop is introduced, and a higher tilt state is reached, the entropy decreases. The form of the transition rates that we are arguing for here, was directly observed in numerical simulations of the three coloring model [17], which is a close relative of the dimer model. The two are equivalent if, in the dimer models, a weight of 2 is attached to each loop formed by bonds that are not covered by dimers.

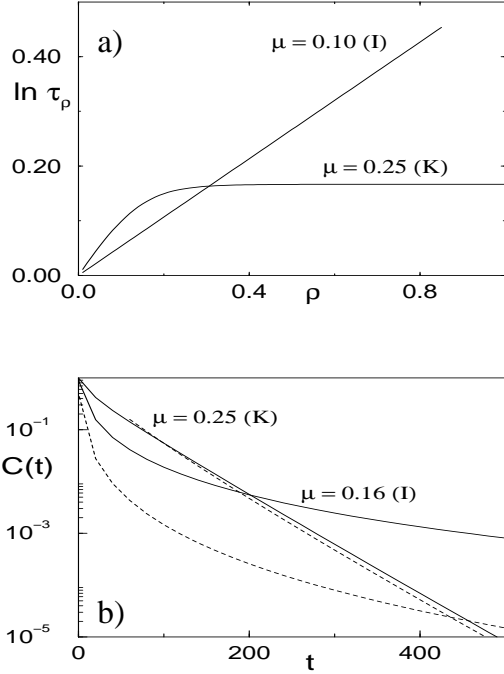


FIG. 2. (a) The time scales for relaxing out of different tilt states  $\rho$  for the *I* and *K* models (scaled by  $L$ ), for values of  $\mu$  below the transition. (b) The tilt-tilt autocorrelation function for the two models. The full line is obtained from Eq. 7 while the dashed line is a result of the saddle point evaluation of Eq. 7.  $L$  was chosen to be 4096 (*I*) and 24 (*K*) to make the time scales comparable. Time is measured in units of  $\Gamma_o^{-1}$ .

The first consequence of the above form of the transition rates is that the time scale of relaxation out of a state with tilt  $\rho$ ,  $\tau_\rho = 1/(W_{\rho-1/L,\rho} + W_{\rho+1/L,\rho})$ , is a *non-decreasing* function of  $\rho$ . The exact expressions for  $\tau_\rho$  (measured in units of  $\Gamma_o^{-1}$ ),

$$\tau_\rho^{-1} = \begin{cases} e^{-\frac{16}{3}\rho\mu L} + e^{-L[\frac{2}{3}\ln 2 + \frac{2}{3}\ln[\cos(\frac{\pi}{3} - \frac{\pi\rho}{3})]]} & (I) \\ e^{-\frac{2}{3}\mu L} + e^{-L[\frac{2}{3}\ln 2 + \frac{2}{3}\ln[\cos(\frac{\pi}{3} - \frac{\pi\rho}{3})]]} & (K) \end{cases}, \quad (5)$$

follow from Eqs. 3 and 4, and they are plotted in Fig. 2. For the *I* model the time scale increases monotonically with  $\rho$  [18], as in the hierarchical models of Palmer *et al.* [19], while in the *K* model an initial rise is followed by saturation beyond  $\rho_{min}$ . Both are in sharp contrast with Langevin dynamics around the equilibrium state, for which the time to relax out of a given macro-state *decreases* the further the order parameter is away from its equilibrium value. (For example, in the Ising model, with Glauber dynamics and in the disordered phase, the relaxation time out of a given magnetization state *decreases* with increasing magnetization.)

The exponential separation between different  $\tau_\rho$ 's for all  $\rho$  in the *I* model, and for  $\rho < \rho_{min}$  in the *K* model, implies that the  $\rho$  dynamics are *trap-like* [20]. By this we

mean that once the system decays out of state  $\rho$  (in time  $\tau_\rho$ ) it quickly loses memory of where it came from.

To quantify the tilt dynamics we compute the tilt-tilt autocorrelation function  $C(t)$ , defined as:

$$C(t) = \frac{\langle \rho(t)\rho(0) \rangle - \langle \rho(0) \rangle^2}{\langle \rho(0)^2 \rangle - \langle \rho(0) \rangle^2}, \quad (6)$$

with the average taken over different histories of  $\rho$ . Assuming trap-like dynamics,

$$C(t) \approx \frac{\sum_\rho (\rho - \langle \rho \rangle)^2 e^{-F(\rho)} e^{-t/\tau_\rho}}{\sum_\rho (\rho - \langle \rho \rangle)^2 e^{-F(\rho)}}, \quad (7)$$

i.e.,  $C(t)$  is an equilibrium weighted average of relaxations out of different  $\rho$  states. Such an approximate model works very well when checked against numerical simulations of the three-coloring model [17].

The asymptotic decay of the autocorrelation functions obtained from Eq. 7 can be extracted from a saddle point analysis of the sum and using a quadratic approximation for the entropy (Eq. 2). The autocorrelation functions obtained from the sum are compared to the saddle point solutions in Fig. 2b. The latter can be used to analyze the asymptotic form of  $C(t)$ , and the dependence of the relaxation time scales on  $\mu$ . In the limit of  $t \rightarrow \infty$ , and up to logarithmic corrections in  $t$ , we find:

$$C(t) \sim \begin{cases} \exp\{-\frac{3}{32}(\frac{\mu_* - \mu}{\mu_*^2})[\ln(\frac{2\mu_* t}{\mu_* - \mu})]^2\} & (I) \\ \exp\{-\frac{t}{e^{2\mu L/3}} - \frac{3\sqrt{3}}{4\pi}[\ln(\frac{t}{e^{2\mu L/3}})]^2\} & (K) \end{cases}, \quad (8)$$

showing that  $C(t)$  has an exponential decay in the *K* model, and a slower than exponential decay in the *I* model. From Eq. 8 we also conclude that the relaxation times scale,  $\tau$ , for the decay of  $C(t)$  to an arbitrary constant  $C_0$ , diverges exponentially as  $\mu \rightarrow \mu_*$  for the *I* model. This is the Vogel-Fulcher type behavior observed in many fragile glass formers. First order corrections to Eq. 8 lead to an even more rapid increase of time scales, with  $\tau/\ln\tau$  diverging as Vogel-Fulcher. In the *K* model the corresponding time scales are exponential in  $\mu$  (Arrhenius form) with no divergence at the transition point.

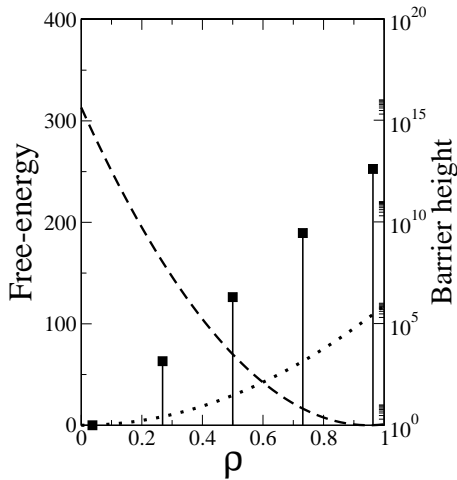


FIG. 3. Barrier height,  $B(\rho)$  (dimensionless) shown as a set of solid lines, and the quadratic approximation to the dimensionless free energies of the  $I$  (dotted line) and  $K$  (dashed line) model;  $\mu$  is chosen close to  $\mu_*$  and  $L = 24$ . Note the logarithmic scale for the barrier height.

The coarse grained dynamics defined by the transition matrix elements, Eqs. 3 and 4, were argued to follow from the nonlocal loop dynamics of the dimer models. From this form of the  $W$ -matrix all the conclusions about critical dynamics of the  $I$  and  $K$  model are derived. We have confirmed this picture in considerable detail in simulations of the three coloring model [21,22], which, as discussed earlier, is the loop weighted dimer model. The loop weights are not expected to affect the qualitative features of the energy and entropy functionals. Indeed, the measured  $\tau_\rho$  for the  $I$  and  $K$  cases of the three-coloring model compare very well [21,22] to the analytical form plotted in Fig. 2. Similarly, the tilt-tilt correlations show exponential decay in the  $K$  model [22] and sub-exponential decay in the  $I$  model [21,22] as expected from the analysis presented in this paper. The numerical evidence for Vogel-Fulcher type divergence of the relaxation time scale in the  $I$  model was reported previously [21].

The origin of the difference in the dynamical behavior of the  $I$  and  $K$  models can be traced back to the interplay between the free energy and the dynamical barriers. The transition rates presented in Eqs. 3 and 4, can be interpreted in terms of a barrier  $B(\rho) = e^{(S(\rho-1/L)-S(\rho))}$  dividing the usual Metropolis rates defined in terms of the free energy and leading to Langevin dynamics [19]. These barriers increase exponentially with  $\rho$  as illustrated in Fig. 3. Dynamics of the order parameter can be viewed as relaxation in the free energy well in the presence of

these barriers (see Fig. 3).

In the  $I$  model the free-energy minimum is centered at  $\rho = 0$  for all values of  $\mu$ . The well gets shallower as  $\mu_*$  is approached implying that the system explores larger and larger barriers leading to a divergent relaxation time scale. In the  $K$  model, the minimum itself shifts to larger values of  $\rho$  and regions of increasing barrier heights ( $\rho_{min} \simeq 1$  in Fig. 3). The dynamics is then completely dominated by a single time scale determined by the barrier at  $\rho_{min}$ .

In conclusion, we have shown that classical dimer models with loop dynamics are an interesting model system for studying glass-like dynamical arrest close to a critical point. Our analysis shows that the jammed nature of the dimer states plays a crucial role in determining the nature of relaxation processes. To quantify how this is reflected in the relaxation time scales we introduced an effective dynamical model based on the master equation for the order parameter. We expect that similar ideas can be carried over to the investigations of hard sphere systems which are of direct relevance to colloidal experiments [3].

Useful conversations with S. Torquato are acknowledged. This work was supported by the NSF DMR-9815986 (DD, BC) and NSF DMR-9984471 (JK).

- 
- [1] S. F. Edwards and D. V. Grinev, in *Jamming and Rheology: Constrained Dynamics on Microscopic and Macroscopic Scales*, eds A. J. Liu and S. R. Nagel, (Taylor and Francis, New York, 2001).
  - [2] C.S. O'Hearn, S.A. Langer, A.J. Liu and S.R. Nagel, Phys. Rev. Lett. **86**, 111, (2001) .
  - [3] V. Trappe *et al.*, Nature **411**, 772 (2001).
  - [4] S. Torquato and F.H. Stillinger, J. Phys. Chem. B **105**, 11849 (2001).
  - [5] L. Santen and W. Krauth, Nature **405**, 550 (2000).
  - [6] J.F. Nagle, C.S.O. Yokoi, and S.M. Bhattacharjee, in *Phase transitions and Critical Phenomena*, eds C. Domb and J.L. Lebowitz, Vol. 13, p. 235 (Academic Press, 1989).
  - [7] C.L. Henley, J. Stat. Phys. **89**, 483 (1997).
  - [8] P.C. Hohenberg and B.I. Halperin, Rev. Mod. Phys. **49**, 435 (1977).
  - [9] C.A. Angell, J. Phys. Chem. **49**, 863 (1988).
  - [10] P.W. Kasteleyn, J. Math. Phys. **4**, 287 (1963).
  - [11] H.W.J. Blöte and H.J. Hilhorst, J.Phys. A **15**, L631 (1982).
  - [12] The components of the tilt along the three lattice directions of the triangular lattice are subject to two constraints. One arising from the conservation of the total dimer number ( $= L^2$ ) and the other from periodic boundary conditions which force two of the components to be equal.
  - [13] A. Dhar, P. Chaudhuri and C. Dasgupta, Phys. Rev. B

- 61**, 6227 (2000).
- [14] H. Yin and B. Chakraborty, Phys. Rev. Lett. **86**, 2058 (2001), and Phys. Rev. E **65**, 036119 (2002).
  - [15] W. Krauth and R. Moessner, cond-mat/0206177.
  - [16] In the  $K$  model, only updates of  $(0, 1)$  loops involve an energy change.
  - [17] D. Das, J. Kondev and B. Chakraborty, cond-mat/0112281.
  - [18] Since the phase transition occurs along the metastable branch in the  $I$  model, the range of  $\rho$ 's participating in the dynamics is restricted to  $\rho \leq \rho_{max}$ . The free energy has a maximum at  $\rho_{max}$  which vanishes as  $\mu \rightarrow \mu_*$  and scales with the system size.
  - [19] R.G. Palmer, D.L. Stein, E. Abrahams and P.W. Anderson, Phys. Rev. Lett. **53**, 958 (1984); S. Teitel, Phys. Rev. Lett. **60**, 1154 (1988).
  - [20] C. Monthus and J-P. Bouchaud, J.Phys. A **29**, 3847 (1996).
  - [21] B. Chakraborty, D. Das and J. Kondev, European Physical Journal E, 2002 (to appear).
  - [22] B. Chakraborty, D. Das and J. Kondev, Physica A, 2002 (to appear), and unpublished.